



Selective [2 + 1 + 1] Fragmentation of P₄ by heteroleptic Metallasilylenes

Juliane Schoening,^[a] Alexander Gehlhaar,^[a] Christoph Wölper,^[a] and Stephan Schulz*^[a]

Abstract: Small-molecule activation by low-valent main-group element compounds is of general interest. We here report the synthesis and characterization (¹H, ¹³C, ²⁹Si NMR, IR, sc-XRD) of heteroleptic metallasilylenes L¹(Cl)MSiL² (M=Al **1**, Ga **2**, L¹=HC[C(Me)NDipp]₂, Dipp=2,6-ⁱPr₂C₆H₃; L²=PhC(N^tBu)₂). Their electronic nature was analyzed by quantum chemical compu-

tations, while their promising potential in small-molecule activation was demonstrated in reactions with P₄, which occurred with unprecedented [2 + 1 + 1] fragmentation of the P₄ tetrahedron and formation of L¹(Cl)MPSi(L²)PPSi(L²)PM(Cl)L¹ (M=Al **3**, Ga **4**).

Small-molecule activation plays a central role in catalysis.^[1] In recent years, the use of main-group-element compounds that exhibit transition-metal-like behavior have become increasingly popular.^[2] Carbene-type divalent tetrylenes, in particular silylenes, with low-lying (unoccupied) acceptor and high-lying (occupied) donor orbitals have been demonstrated to be suitable candidates for the activation of small molecules such as H₂, CO or CO₂,^[3] and in catalytic transformations.^[4,5] The activation of white phosphorus is also of fundamental interest in order to further convert P₄ into valuable organophosphorus compounds. In addition, activation as well as fragmentation of P₄ was reported in reactions with cyclic and acyclic (alkyl)(amino)carbenes as well as with anionic dicarbenes and mesoionic carbenes,^[6] as well as disilenes, tetrylenes,^[7] and group 13 carbenoids (Figure 1).^[8] Cyclic and acyclic silylenes reacted with P₄ to Si_nP₄ cages (n=1 (**I**), 2 (**II**)),^[9] whereas amidinato-substituted silylenes (PhC(N^tBu)₂SiCl) and PhC(N^tBu)₂SiN(SiMe₃)₂ yielded a Si₂P₂ four-membered ring (**III**) and an acyclic P₄ chain (**IV**), respectively.^[10] Driess et al. recently reported on the degradation of P₄, yielding an NHSi-stabilized zero-valent P₂ complex (**V**) and its functionalization by small molecules.^[11]

We recently reported the first room temperature stable silylene carbonyl complex [L¹(Br)Ga]₂SiCO.^[12a] Homoleptic [L¹(Br)Ga]₂Si: could not be isolated and was only proposed as reaction intermediate. To further elucidate the electronic effect

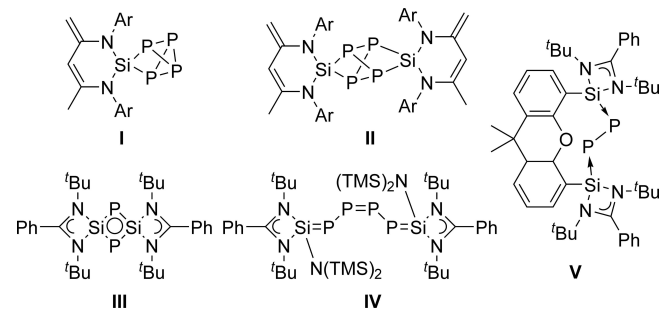
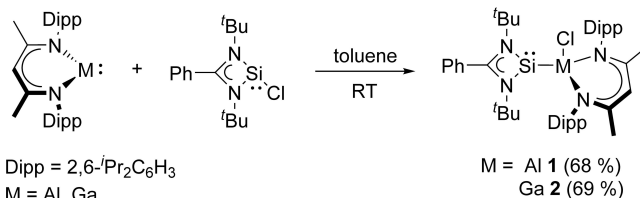


Figure 1. P₄ activation products formed in reactions of silylenes.

of the L¹(Br)M ligand, we became interested in heteroleptic metallasilylenes and herein report on the synthesis of L¹(Cl)MSiL² (M=Al **1**, Ga **2**). Their electronic structures were analyzed by quantum chemical computations, and their reactions with white phosphorus, which proceeded with unforeseen [2 + 1 + 1] fragmentation of the P₄ tetrahedron, are reported.

Group 13 diyls L¹M (M=Al, Ga)^[13] react with silylene L²SiCl^[14] in benzene or toluene at ambient temperature with oxidative addition and formation of L²SiM(Cl)L¹ (M=Al **1**, Ga **2**, Scheme 1). Complexes **1** and **2** are soluble in benzene and toluene, but readily decompose in polar solvents such as CH₂Cl₂ at ambient temperature. ¹H and ¹³C NMR spectra of **1** and **2** (Tables S1 and S2 in the Supporting Information) show the characteristic resonances of the β-diketiminate (L¹) and the amidinate (L²)



Scheme 1. Synthesis of heteroleptic metallasilylenes **1** and **2**.

[a] J. Schoening, A. Gehlhaar, Dr. C. Wölper, Prof. Dr. S. Schulz

Institute for Inorganic Chemistry and Center for
Nanointegration Duisburg-Essen (Cenide)

University of Duisburg-Essen

Universitätstrasse 5–7, 45117 Essen (Germany)
E-mail: stephan.schulz@uni-due.de

Supporting information for this article is available on the WWW under
<https://doi.org/10.1002/chem.202201031>

© 2022 The Authors. Chemistry - A European Journal published by Wiley-VCH GmbH. This is an open access article under the terms of the Creative Commons Attribution Non-Commercial License, which permits use, distribution and reproduction in any medium, provided the original work is properly cited and is not used for commercial purposes.

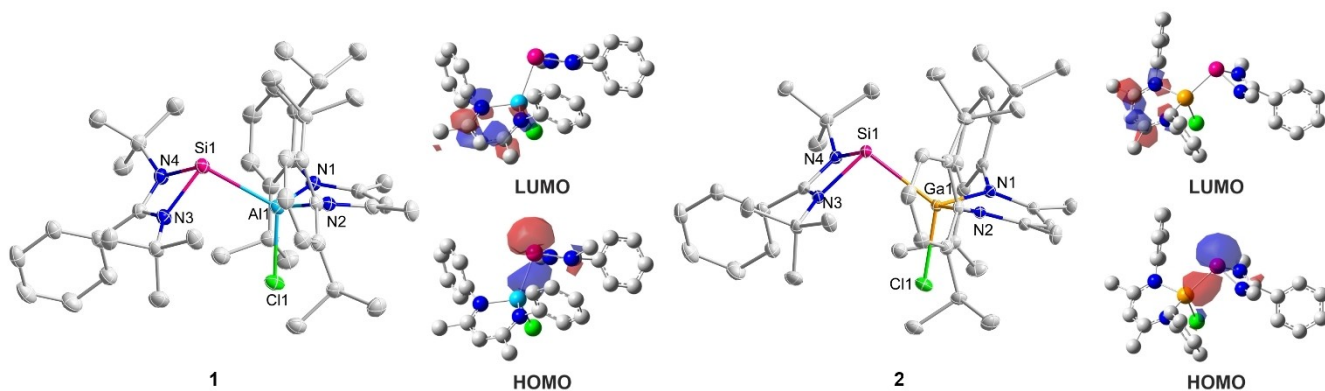


Figure 2. Molecular structure and frontier orbitals (isovalue 0.05) of metallasilylenes **1** (left) and **2** (right). Displacement ellipsoids are at 50% probability; hydrogen atoms are omitted for clarity; 'Pr' groups are omitted, and 'Bu' groups are reduced to C for clarity in calculated structures. Selected bond lengths [Å] and angles [°]: **1**: Si1–Al1 2.5620(6), Al1–Cl1 2.2043(6), Si1–N3 1.8760(12), Si1–N4 1.8888(13), Al1–N1 1.9176(13), Al1–N2 1.9505(13), N3–Si1–N4 69.10(6), N1–Al1–N2 94.39(5), Si1–Al1–Cl1 117.81(2); **2**: Si1–Ga1 2.5170(4), Ga1–Cl1 2.2837(4), Si1–N3 1.8686(9), Si1–N4 1.8859(19), Ga1–N1 1.9810(9), Ga1–N2 2.0183(9), N3–Si1–N4 69.38(4), N1–Ga1–N2 92.65(4), Si1–Ga1–Cl1 119.136(11).

ligands; the ^{29}Si NMR spectra show singlets at 93.0 ppm for **1** and 65.1 ppm for **2**.

Single crystals of **1** and **2**, which crystallize in the triclinic space group $P\bar{1}$, were obtained from toluene solutions upon storage at -18°C for 12 h (Figure 2). The four-membered SiNCN rings are planar, whereas the six-membered MN_2C_3 rings ($\text{M} = \text{Al, Ga}$) adopt boat-type conformations. The Si–M bond lengths (2.5620(6) Å **1**, 2.5170(4) Å **2**) are best described as single bonds,^[15] even though they are longer than the corresponding sums of covalent radii (Si–Al 2.42 Å, Si–Ga 2.40 Å).^[16] The Al–Cl bond (2.2043(6) Å) is shorter than the Ga–Cl bond (2.28370(4) Å), but both are in the range of typical M–Cl bond lengths.^[17] The N–Si–N bond angles (**1** 69.1(1)°, **2** 69.4(1)°) are fairly identical with those in L^2SiCl **A** (68.35(8)°)^[14] and silylenes **B**–**H** (Figure 3),^[18] whereas the M–Si–N bond angles (**1** 100.5(1)°, 103.9(1)°, **2** 99.0(1)°, 101.9(1)°) are wider than Cl–Si–N bond angles in L^2SiCl (95.82(6)°; 96.56(6)°) due to the sterically more demanding $\text{L}^1(\text{Cl})\text{M}$ ligands.

The electronic structures of **1** and **2** were analyzed with ORCA (version 5.0)^[19] and the NBO program package (version 7.0.10)^[20] at the 6-311G(d,p)^[21] level of theory (def2-TZVP for E>Ne)^[22] using the atom-pairwise dispersion correction with the Becke-Johnson damping scheme (D3BJ)^[23] with the B3LYP^[24] functional. The HOMOs of **1** and **2** are almost exclusively reflected by the electron lone pair of the silicon atom and the Si–M bonds, while the LUMOs are located at the β -diketiminate ligands (Figure 2). The smaller HOMO–LUMO gap of **1** (2.81 eV

compared to **2** (3.52 eV) reflects the more electropositive nature of Al versus Ga, indicating a higher reactivity of **1** compared to **2**. Natural bond orbital (NBO) analyses (Table S5) showed that the M–Si bond in **1** (Si: 59.6%; Al: 40.4%) is more polarized than in **2** (Si: 48.7%; Ga: 51.3%), resulting from the more electropositive character of Al. This also agrees with the observed natural charges for the Si (+0.33 **1**, +0.50 **2**) and the group 13 metals M (Al +1.47 **1**, Ga +1.17 **2**).

Heteroleptic metallasilylenes **1** and **2** are expected to be reactive species due to the presence of a Lewis basic (Si) and Lewis acidic (M) center. To evaluate the influence of the $\text{L}(\text{X})\text{M}$ ligand on the electronic nature of **1** and **2**, we compared both silylenes with structurally related heteroleptic and homoleptic acyclic silylenes **A**–**H** (Figure 3). Replacing the $\text{L}^1(\text{Cl})\text{M}$ ligand in **1** and **2** by $\text{E}(\text{SiMe}_3)_3$ ligands ($\text{E} = \text{C E, Si F}$) increases the natural partial charge of Si, following the trend of electronegativity ($\text{E} = +1.10\text{e}$, $\text{F} = +0.73\text{e}$), and polarizes the Si–E bond, whereas introduction of a second $\text{L}^1(\text{X})\text{M}$ ligand results in a reversed polarity of the silicon center in the homoleptic metallasilylenes [$\text{L}^1(\text{X})\text{M}]_2\text{Si}$: ($\text{M} = \text{Ga, } -0.13\text{e}$ **G**; $\text{Al, } -0.45\text{e}$ **H**), with marginal changes in bond polarity. In addition, the partial charge of the Si atom increases significantly upon replacement of the Ga atom by a more electropositive Al atom. Wiberg bond indices (WBI) and Mayer bond orders (MBO) are in good agreement and point to rather covalent Si–M bonds in **G** and **H**. Replacing the $\text{L}^1(\text{Cl})\text{M}$ ligand in **1** and **2** by electronegative halide (Cl **A**, Br **B**) and $\text{E}(\text{SiMe}_3)_2$ ligands ($\text{E} = \text{N C, P D}$) results in an increase of the natural partial charges on the Si atom and further polarizes the Si–E bond to a comparable value as observed for **E**. Furthermore, the HOMO–LUMO gaps increase, with **A** and **B** showing the largest energy gap of the investigated compounds. Table 1 summarizes selected electronic properties of silylenes **1**, **2** and **A**–**H**.

With metallasilylenes **1** and **2** in hand, we became interested in their reactivity toward white phosphorus. In marked contrast to reactions of amidinate-substituted silylenes $\text{PhC}(\text{N}^t\text{Bu})_2\text{SiCl}$ **A** and $\text{PhC}(\text{N}^t\text{Bu})_2\text{SiN}(\text{SiMe}_3)_2$ **C** with P_4 ,^[10] which

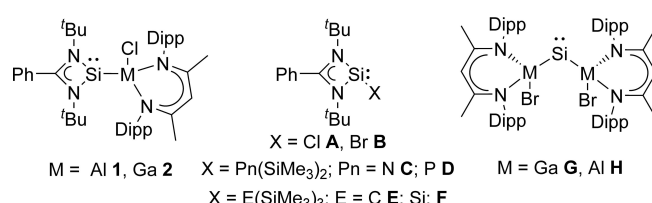
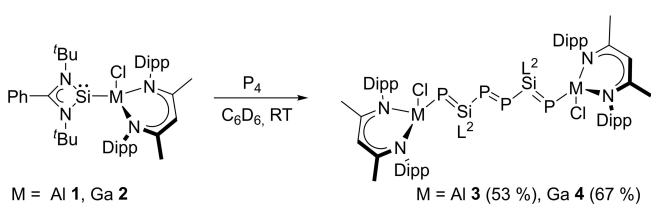


Figure 3. Silylenes **1**, **2** and **A**–**H** selected for comparison.

Table 1. Natural partial charge of Si, HOMO-LUMO ($\Delta E_{\text{HOMO-LUMO}}$) and singlet-triplet energy gaps (ΔE_{ST}) of acyclic silylenes 1, 2 and A–H.

	Q(Si) [e]	$\sigma(\text{Si}–\text{E})$ contribution	$\Delta E_{\text{HOMO-LUMO}}$ [eV]	ΔE_{ST} [kcal mol^{-1}]
A ^[14a]	+0.97	Si(20.4%)-Cl(79.6%)	4.37	-51.78
B ^[25]	+0.93	Si(22.5%)-Br(77.5%)	4.39	-50.50
C ^[26]	+1.15	Si(12.5%)-N(87.5%)	3.88	-38.93
D ^[27]	+0.83	Si(31.2%)-P(68.8%)	3.82	-40.28
E ^[28]	+1.10	Si(20.0%)-C(80.0%)	3.74	-29.51
F ^[29]	+0.73	Si(39.0%)-Si(61.0%)	3.61	-42.43
1	+0.33	Si(59.6%)-Al(40.4%)	2.81	-36.36
2	+0.50	Si(48.7%)-Ga- (51.3%)	3.52	-49.14
G ^[12a]	-0.13	Si(53.4%)-Ga- (46.6%)	2.17	-1.77
H	-0.45	Si(62.6%)-Al(37.4%)	1.93	+4.81

gave the four-membered Si_2P_2 ring (**III**) and the acyclic Si_2P_4 chain (**IV**), **1** and **2** reacted with P_4 in 2:1 molar ratio. After short heating to reflux, dark green solutions were formed, which according to *in situ* ^1H and ^{31}P NMR spectroscopy studies only contained a single species, which was finally identified as the unique $[2+1+1]$ fragmentation products $\text{L}^1(\text{Cl})\text{MPSi}(\text{L}^2)\text{PPSi}(\text{L}^2)\text{PM}(\text{Cl})\text{L}^1$ ($\text{M} = \text{Al}$ **3**, Ga **4**) containing two P_2 unit and one P_2 unit.



Scheme 2. Synthesis of compounds **3** and **4**.

Compounds **3** and **4** were isolated in good yields after storage at ambient temperature for 12 h (Scheme 2). Their ^1H and ^{13}C NMR spectra show the expected resonances of the ligands (L^1 , L^2), whereas no ^{29}Si NMR signal could be recorded. The ^{31}P NMR spectra each show two signals for the P_2 unit (**3** 641.7 ppm; **4** 629.4 ppm), and the chemical shifts agree to values previously reported for diphosphenes^[30a] including silyl-substituted diphosphenes $\text{R}_3\text{SiPPSiR}_3$ ($\text{R} = {^t\text{Bu}}\text{Si}$, $\delta = 818.1$ ppm;^[30b] Me_3Si , $\delta = 735.0$ ppm^[30c]). In addition, the single phosphorus atoms gave resonances at -262.7 ppm (**3**) and -253.6 ppm (**4**), which are in a comparable region observed for compounds with monophosphide anions such as $\text{L}^2\text{Si}[\text{N}(2\text{-py})\text{Me}]\text{P}(\text{SiL}^1)\text{P}_3\text{SiL}^2[\text{N}(2\text{-py})\text{Me}]$ (-261.4 ppm).^[40]

Dark green crystals of **3** (Figure 4A) and **4** (Figure S17A), which crystallize in the triclinic space group $P\bar{1}$ with one molecule in the unit cell, were grown from benzene solutions upon storage at ambient temperature. Central structural motif in both compounds is the unique eight-membered chain with planar $\text{M}-\text{P}=\text{Si}-\text{P}=\text{P}-\text{Si}=\text{P}-\text{M}$ units and rather localized alternating single ($\text{M}-\text{P}$, $\text{Si}-\text{P}$) and double bonds ($\text{P}=\text{Si}$, $\text{P}=\text{P}$). The $\text{P}2-\text{P}2\text{a}$ bond lengths ($2.0270(10)$ Å **3**; $2.0323(7)$ Å **4**) are at the upper range of $\text{P}-\text{P}$ double bonds (1.985 – 2.050 Å)^[7c,31] and slightly shorter than the $\text{P}-\text{P}$ double bond in $\text{L}^2\text{Si}=\text{P}-\text{P}=\text{P}-\text{SiL}^2$ **IV** ($2.0559(7)$ Å)^[10a] and in $\text{L}^2\text{Si}[\text{N}(2\text{-py})\text{Me}]\text{P}(\text{SiL}^1)\text{P}_3\text{SiL}^2[\text{N}(2\text{-py})\text{Me}]$ ($2.0577(4)$ Å),^[40] whereas the $\text{P}-\text{P}$ bond in zero-valent P_2 complex **V** is substantially elongated ($2.2369(8)$ Å).^[11] The $\text{Si}1-\text{P}2$ bond lengths ($2.3091(7)$ Å **3**, $2.3018(3)$ Å **4**) are in the range of typical $\text{Si}-\text{P}$ single bonds and agree with the calculated single bond value of 2.27 Å,^[19] whereas the $\text{Si}1-\text{P}1$ bonds ($2.1010(4)$ Å **3**; $2.1127(4)$ Å **4**), which perfectly fit to the calculated sum of covalent radii for a $\text{Si}-\text{P}$ double bond (2.09 Å),^[19,32] are identical to that reported for phosphasilene (${^t\text{Bu}}_2\text{MeSi}_2\text{SiPMes}^*$ ($2.1114(7)$ Å; $\text{Mes}^* = 2,4,6\text{-Me}_3\text{C}_6\text{H}_2$)^[33] and in

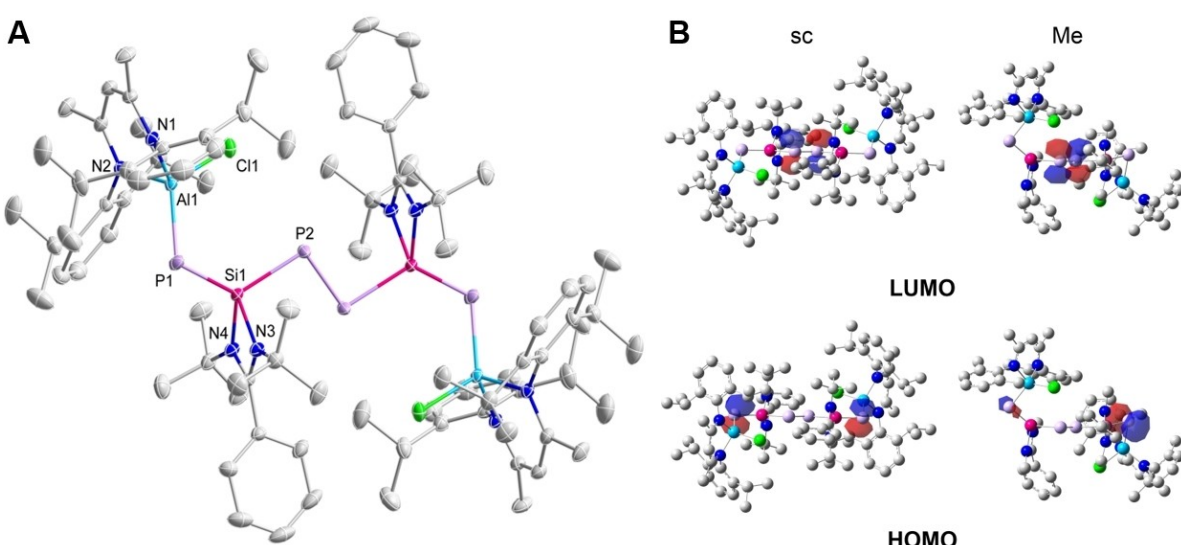


Figure 4. A) Molecular structure and B) frontier orbitals (isovalue 0.05) of compound **3**. Displacement ellipsoids are at 50 % probability; hydrogen atoms, disorders and solvent molecules (benzene) are omitted for clarity. Selected bond lengths [Å] and angles [°]: **3**: $\text{P}2-\text{P}2\text{a}$ 2.0270(10), $\text{Si}1-\text{P}1$ 2.1010(4), $\text{Si}1-\text{P}2$ 2.3091(7), $\text{Al}1-\text{P}1$ 2.2622(4), $\text{P}1-\text{Si}1-\text{P}2$ 125.65(2), $\text{P}2\text{a}-\text{P}2-\text{Si}1$ 100.38(4), $\text{Si}1-\text{P}1-\text{Al}1$ 107.172(16); **4**: $\text{P}2-\text{P}2\text{a}$ 2.0323(7), $\text{Si}1-\text{P}1$ 2.1127(4), $\text{Si}1-\text{P}2$ 2.3018(7), $\text{Ga}1-\text{P}1$ 2.2510(3), $\text{P}1-\text{Si}1-\text{P}2$ 125.763(17), $\text{P}2\text{a}-\text{P}2-\text{Si}1$ 99.36(2), $\text{Si}1-\text{P}1-\text{Ga}1$ 104.770(14).

$\text{L}^2\text{Si}[\text{N}(2\text{-py})\text{Me}] \text{P}(\text{SiL}^1)\text{P}_3\text{SiL}^2[\text{N}(2\text{-py})\text{Me}]$ ($2.1157(4)$ Å).^[40] In contrast, those observed for complexes **V** ($2.1307(7)$, $2.1263(7)$ Å)^[11] and **IV** ($2.1602(12)$ Å),^[10a] which contains a rather delocalized π -electron system within the six-membered SiP_4Si chain, are slightly elongated. In contrast, phosphasilene ${}^1\text{Bu}(\text{Dipp})\text{FSiPSi}(\text{Dipp}){}^1\text{Bu}$ exhibited a shorter P–Si bond ($2.053(2)$ Å).^[34] The M–P bonds ($\text{M}=\text{Al}$ $2.2622(4)$ Å **3**, Ga $2.2510(3)$ Å **4**) are shorter than the calculated single bonds (Al–P 2.37 Å; Ga–P 2.35 Å)^[19] and comparable to Ga–P single bonds in gallaphosphene $\text{L}^1\text{GaPGa}(\text{Cl})\text{L}^1$ ($2.2688(5)$ Å).^[35]

The first step in the nucleophilic activation of P_4 by silylenes typically occurs with cleavage of one P–P bond by σ -bond metathesis.^[36] However, understanding the fragmentation process of the subsequent P–P bond cleavage reactions by trapping as-formed P_1 - and P_3 -containing species is challenging due to their high reactivity.^[37] However, P_4 undergoes [2+2] fragmentation, yielding activated P_2 -containing species **N** or **O**, or [3+1] fragmentation giving the activated P_1 -containing species **Q** and two possible P_3 -containing species **P** or **R** (Figure 5). [3+1]-type fragmentation of white phosphorus was previously reported for reactions with lutetacyclopentadienes,^[38] which occurred by a step-by-step process of three P–P bond cleavages and four P–C bond formation, as well as with a diboraallene.^[39] While this work was under revision, Roesky et al. reported [3+1] fragmentation of the P_4 tetrahedron by treating the amido(pyridyl)-functionalized silylene [$\text{L}^2\text{Si}[\text{N}(2\text{-py})\text{Me}]$] with [$\text{L}^1\text{Si}(\eta^2\text{-P}_4)$.^[40] The formation of the hexatriene-type chains in complexes **3** and **4** probably follows a comparable reaction mechanism as described by Roesky et al., even though we finally isolated the [2+1+1] fragmentation product, in which threefold P–P single bond breakage of two P atoms of the starting P_4 molecule occurred. This is without precedence in both main group metal and transition metal mediated P_4 activation.

NBO analyses were performed to get further insight into the electronic structure of the $\text{M}_2\text{P}_4\text{Si}_2$ chain. Due to the large ligand framework in **3** and **4**, we performed single-point calculations with the coordinates as found in the solid-state structures (**3**^{sc}, **4**^{sc}) and also replaced the ${}^1\text{Pr}$ by smaller Me groups (**3**^{Me}, **4**^{Me}). The resulting frontier orbitals of both calculations agreed well with each other, with the HOMOs being reflected by the P1 electron lone pair, while the LUMOs are represented by the antibonding P2–P2a π^* orbital. However, **3**^{Me} and **4**^{Me} show rotation about the Si–P bond, resulting in L^1M being nearly perpendicular to the SiP_2Si plane (Figures 4B and S17B).

The WBIs for the central chain (M1–P1 av. 0.89 (**3**), 0.98 (**4**); P1–Si1 1.46 (**3**), 1.42 (**4**); Si1–P2 0.90 (**3**), 0.90 (**4**); P2–P2a 1.85

(**3**), 1.85 (**4**)) emphasize alternating localized single and double bonds. The natural partial charges ($\text{M1} + 1.62\text{e}$ (**3**), $+1.38\text{e}$ (**4**); $\text{P1} - 1.05\text{e}$ (**3**), -0.94e (**4**); $\text{Si1} + 1.30\text{e}$ (**3**), $+1.31\text{e}$ (**4**); $\text{P2} - 0.21\text{e}$ (**3**), -0.19e (**4**)) show bond polarizations toward the P atoms, while the slightly different values result from the broken symmetry in **3**^{Me} and **4**^{Me} due to the rotation (Table S7). Although these data suggest a rather localized electronic system with alternating single and double bonds, some delocalization corrections are observed in the second order perturbation theory analysis in NBO basis. The interactions observed within the eight-membered chains ($\text{M} = \text{Al}$ **3**, Ga **4**) stabilize the molecular units ($n_{\text{P1}}^{\text{a}} \rightarrow n_{1^*}^{\text{M1}}$ 12.1 (**3**), av. 16.5 (**4**); $n_{\text{P1}}^{\text{a}} \rightarrow \sigma^*_{\text{Si–P2}}$ 10.1 (**3**), 9.0 (**4**); $\sigma_{\text{M1–P1}} \rightarrow n_{1^*}^{\text{Si}}$ 11.1 (**3**), 10.0 (**4**) kcal mol⁻¹), whereas the interactions between the π systems are comparatively small ($\pi_{\text{P2–P2a}} \rightarrow n_{2^*}^{\text{Si}}$ 1.3 (**3**), 2.1 (**4**); $\pi_{\text{P2–P2a}} \rightarrow \pi^*_{\text{Si–P1}}$ 6.0 (**3**), 5.5 (**4**) kcal mol⁻¹) except for the $\pi_{\text{Si–P1}} \rightarrow n_{2^*}^{\text{M1}}$ interaction (16.7 (**3**), 13.4 (**4**) kcal mol⁻¹).

To conclude, heteroleptic metallasilylenes $\text{L}^1(\text{Cl})\text{MSiL}^2$ ($\text{M} = \text{Al}$ **1**, Ga **2**) show HOMO–LUMO gaps ($\Delta E_{\text{HOMO–LUMO}}$) in between those observed for “classical” heteroleptic amidinate-substituted silylenes $\text{L}^2\text{Si}(\text{X})$ and homoleptic metallasilylenes [$\text{L}^1(\text{X})\text{M}_2\text{Si}$:]. They react with white phosphorus with degradation of the P_4 tetrahedron to $\text{L}^1(\text{Cl})\text{MP}=\text{Si}(\text{L}^2)\text{P}=\text{PSi}(\text{L}^2)=\text{PM}(\text{Cl})\text{L}^1$ ($\text{M} = \text{Al}$ **3**, Ga **4**), containing two P_1 and one P_2 units. The capability of **3** and **4** to serve as starting reagents for a controlled mono- and diphosphorus anion transfer and the synthesis of valuable organophosphorus compounds is currently under investigation.

Deposition Numbers 2161455 (1), 2161456 (2), 2161937 (3), and 2161938 (4) contain the supplementary crystallographic data for this paper. These data are provided free of charge by the joint Cambridge Crystallographic Data Centre and Fachinformationszentrum Karlsruhe Access Structures service.

Acknowledgements

We acknowledge financial support by the DFG (SCHU1069/26-1) and the University of Duisburg-Essen. Open Access funding enabled and organized by Projekt DEAL.

Conflict of Interest

The authors declare no conflict of interest.

Data Availability Statement

The data that support the findings of this study are available in the supplementary material of this article.

Keywords: P_4 activation · quantum chemical calculations · silylene · X-ray diffraction

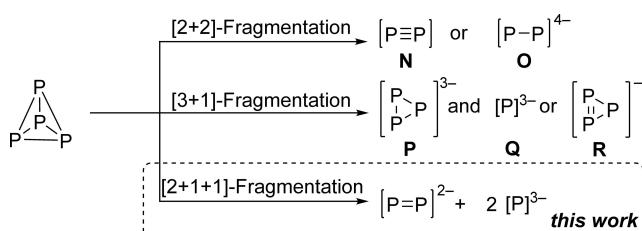


Figure 5. Fragmentation reactions of white phosphorus.

- [3] S. Fujimori, S. Inoue, *Eur. J. Inorg. Chem.* **2020**, 3131–3142.
- [4] a) R. L. Melen, *Science* **2019**, 363, 479–484; b) C. Weetman, S. Inoue, *ChemCatChem* **2018**, 10, 4213–4228.
- [5] a) E. M. Leitao, T. Jurca, I. Manners, *Nat. Chem.* **2013**, 5, 817–829; b) S. Yadav, S. Saha, S. S. Sen, *ChemCatChem* **2016**, 8, 486–501; c) T. Chu, G. I. Nikonorov, *Chem. Rev.* **2018**, 118, 3608–3680; d) T. J. Hadlington, M. Driess, C. Jones, *Chem. Soc. Rev.* **2018**, 47, 4176–4197.
- [6] a) J. D. Masuda, W. W. Schoeller, B. Donnadieu, G. Bertrand, *Angew. Chem. Int. Ed.* **2007**, 46, 7052–7055; *Angew. Chem.* **2007**, 119, 7182–7185; b) O. Back, G. Kuchenbeiser, B. Donnadieu, G. Bertrand, *Angew. Chem. Int. Ed.* **2009**, 48, 5530–5533; *Angew. Chem.* **2009**, 121, 5638–5641; c) D. Rottschäfer, S. Blomeyer, B. Neumann, H.-G. Stammle, R. S. Ghadwal, *Chem. Sci.* **2019**, 10, 11078–11085.
- [7] a) M. Driess, A. D. Fanta, D. R. Powell, R. West, *Angew. Chem. Int. Ed. Engl.* **1989**, 28, 1038–1040; *Angew. Chem.* **1989**, 101, 1087–1088; b) S. S. Sen, S. Khan, H. W. Roesky, D. Kratzert, K. Meindl, J. Henn, D. Stalke, J.-P. Demers, A. Lange, *Angew. Chem. Int. Ed.* **2011**, 50, 2322–2325; *Angew. Chem.* **2011**, 123, 2370–2373; c) S. Khan, R. Michel, S. S. Sen, H. W. Roesky, D. Stalke, *Angew. Chem. Int. Ed.* **2011**, 50, 11786–11789; *Angew. Chem.* **2011**, 123, 11990–11993; d) J. W. Dube, C. M. E. Graham, C. L. B. Macdonald, Z. D. Brown, P. P. Power, P. J. Ragogna, *Chem. Eur. J.* **2014**, 20, 6739–6744; e) D. Sarkar, C. Weetman, D. Munz, S. Inoue, *Angew. Chem. Int. Ed.* **2021**, 60, 3519–3523; *Angew. Chem.* **2021**, 133, 3561–3565.
- [8] a) Y. Peng, H. Fan, H. Zhu, H. W. Roesky, J. Magull, C. E. Hughes, *Angew. Chem. Int. Ed.* **2004**, 43, 3443–3445; *Angew. Chem.* **2004**, 116, 3525–3527; b) C. Dohmeier, H. Schnöckel, C. Robl, U. Schneider, R. Ahlrichs, *Angew. Chem. Int. Ed.* **1994**, 33, 199–200; *Angew. Chem.* **1994**, 106, 225–227; c) W. Uhl, M. Benter, *Chem. Commun.* **2000**, 771–772; d) A. R. Fox, R. J. Wright, E. Rivard, P. P. Power, *Angew. Chem. Int. Ed.* **2005**, 44, 7729–7733; *Angew. Chem.* **2005**, 117, 7907–7911; e) F. Hennersdorf, J. Frötschel, J. J. Weigand, *J. Am. Chem. Soc.* **2017**, 139, 14592–14604.
- [9] a) Y. Xiong, S. Yao, M. Brym, M. Driess, *Angew. Chem. Int. Ed.* **2007**, 46, 4511–4513; *Angew. Chem.* **2007**, 119, 4595–4597; b) I. Alvarado-Beltran, A. Baceiredo, N. Saffon-Merceron, V. Branchadell, T. Kato, *Angew. Chem. Int. Ed.* **2016**, 55, 16141–16144; *Angew. Chem.* **2016**, 128, 16375–16378; c) D. Reiter, P. Frisch, D. Wendel, F. M. Hörmann, S. Inoue, *Dalton Trans.* **2020**, 49, 7060–7068; d) M. M. D. Roy, M. J. Ferguson, R. McDonald, Y. Zhou, E. Rivard, *Chem. Sci.* **2019**, 10, 6476–6481.
- [10] a) S. S. Sen, S. Khan, H. W. Roesky, D. Kratzert, K. Meindl, J. Henn, D. Stalke, J.-P. Demers, A. Lange, *Angew. Chem. Int. Ed.* **2011**, 50, 2322–2325; *Angew. Chem.* **2011**, 123, 2370–2373; b) S. Khan, R. Michel, S. S. Sen, H. W. Roesky, D. Stalke, *Angew. Chem. Int. Ed.* **2011**, 50, 11786–11789; *Angew. Chem.* **2011**, 123, 11990–11993.
- [11] Y. Wang, T. Szilvási, S. Yao, M. Driess, *Nat. Chem.* **2020**, 12, 801–807.
- [12] a) C. Ganesamoorthy, J. Schoening, C. Wölper, L. Song, P. R. Schreiner, S. Schulz, *Nat. Chem.* **2020**, 12, 608–614; b) D. Reiter, R. Holzner, A. Porzelt, P. Frisch, S. Inoue, *Nat. Chem.* **2020**, 12, 1131–1135; c) T. Sergejeva, D. Mandal, D. M. Andrade, *Chem. Eur. J.* **2021**, 27, 10601–10609.
- [13] a) N. J. Hardman, B. E. Eichler, P. P. Power, *Chem. Commun.* **2000**, 1991–1992; b) C. Cui, H. W. Roesky, H.-G. Schmidt, M. Noltemeyer, H. Hao, F. Cimpoesu, *Angew. Chem. Int. Ed.* **2000**, 39, 4274–4276; *Angew. Chem.* **2000**, 112, 4444–4446.
- [14] a) C.-W. So, H. W. Roesky, J. Magull, R. B. Oswald, *Angew. Chem. Int. Ed.* **2006**, 45, 3948–3950; *Angew. Chem.* **2006**, 118, 4052–4054; b) S. S. Sen, H. W. Roesky, D. Stern, J. Henn, D. Stalke, *J. Am. Chem. Soc.* **2010**, 132, 1123–1126.
- [15] The CCDC database lists a range of 2.396 to 2.717 Å (mean 2.483 Å, median 2.478 Å) for Si–Al bond lengths and a range of 2.329 to 2.584 Å for Si–Ga bonds (mean 2.442 Å, median 2.439 Å). *Cambridge Structural Database, Version 5.41*, see also: F. H. Allen, *Acta Crystallogr. Sect. B* **2002**, 58, 380–388.
- [16] P. Pyykko, M. Atsumi, *Chem. Eur. J.* **2009**, 15, 12770–12779.
- [17] A search for Al–Cl (only terminal Cl) yielded 1418 hits (4809 bonds) ranging from 1.978 to 2.509 Å with a mean of 2.14(5) Å. A search for Ga–Cl (only terminal Cl) yielded 1330 hits (4504 bonds) ranging from 1.974 to 2.543 Å with a mean of 2.18(5) Å. *Cambridge Structural Database, Version 5.41*, see also: F. H. Allen, *Acta Crystallogr. Sect. B* **2002**, 58, 380–388.
- [18] a) S. Inoue, W. Wang, C. Präsang, M. Asay, E. Irran, M. Driess, *J. Am. Chem. Soc.* **2011**, 133, 2868–2871; b) R. Azhakar, R. S. Ghadwal, H. W. Roesky, H. Wolf, D. Stalke, *Organometallics* **2012**, 31, 4588–4592; c) C.-W. So, H. W. Roesky, P. M. Gurubasavaraj, R. B. Oswald, M. T. Gamer, P. G. Jones, S. Blaurock, *J. Am. Chem. Soc.* **2007**, 129, 12049–12054; d) S. S. Sen, J. Hey, R. Herbst-Irmer, H. W. Roesky, D. Stalke, *J. Am. Chem. Soc.* **2011**, 133, 12311–12316; e) S. Kaufmann, F. Krätschmer, R. Köppe, T. Schon, C. Schoo, P. W. Roesky, *Chem. Sci.* **2020**, 11, 12446–12452; f) R. Azhakar, H. W. Roesky, J. J. Holstein, B. Dittrich, *Eur. J. Inorg. Chem.* **2013**, 2013, 2777–2781; g) R. Azhakar, R. S. Ghadwal, H. W. Roesky, H. Wolf, D. Stalke, *Chem. Commun.* **2012**, 48, 4561–4563; h) M. K. Bisai, V. S. V. S. N. Swamy, T. Das, K. Vanka, R. G. Gonnade, S. S. Sen, *Inorg. Chem.* **2019**, 58, 10536–10542.
- [19] F. Neese, *WIREs Comput. Mol. Sci.* **2018**, 8, e1327.
- [20] E. D. Glendening, J. K. Badenhoop, A. E. Reed, J. E. Carpenter, J. A. Bohmann, C. M. Morales, P. Karafiloglu, C. R. Landis, F. Weinhold, *NBO 7.0, Theoretical Chemistry Institute, University of Wisconsin–Madison*, **2018**.
- [21] R. Krishnan, J. S. Binkley, R. Seeger, J. A. Pople, *J. Chem. Phys.* **1980**, 72, 650.
- [22] F. Weigend, R. Ahlrichs, *Phys. Chem. Chem. Phys.* **2005**, 7, 3297–3305.
- [23] a) S. Grimme, S. Ehrlich, L. Goerigk, *J. Comput. Chem.* **2011**, 32, 1456–1465; b) S. Grimme, J. Antony, S. Ehrlich, H. Krieg, *J. Chem. Phys.* **2010**, 132, 154104.
- [24] J. Tao, J. P. Perdew, V. N. Staroverov, G. E. Scuseria, *Phys. Rev. Lett.* **2003**, 91, 146401.
- [25] H.-X. Yeong, K.-C. Lau, H.-W. Xi, K. H. Lim, C.-W. So, *Inorg. Chem.* **2010**, 49, 371–373.
- [26] S. S. Sen, J. Hey, R. Herbst-Irmer, H. W. Roesky, D. Stalke, *J. Am. Chem. Soc.* **2011**, 133, 12311–12316.
- [27] S. Inoue, W. Wang, C. Präsang, M. Asay, E. Irran, M. Driess, *J. Am. Chem. Soc.* **2011**, 133, 2868–2871.
- [28] R. Azhakar, R. S. Ghadwal, H. W. Roesky, H. Wolf, D. Stalke, *Chem. Commun.* **2012**, 48, 4561–4563.
- [29] M. K. Bisai, V. S. V. S. N. Swamy, T. Das, K. Vanka, R. G. Gonnade, S. S. Sen, *Inorg. Chem.* **2019**, 58, 10536–10542.
- [30] a) H.-P. Schrödel, A. Schmidpeter, *Phosphor. Sulfur Silicon Relat. Elem.* **1997**, 129, 69–76; b) N. Wiberg, A. Wörner, H.-W. Lerner, K. Karaghiosoff, *Z. Naturforsch. B* **2002**, 57, 1027–1035; c) V. Cappello, J. Baumgartner, A. Dransfeld, M. Flock, K. Hassler, *Eur. J. Inorg. Chem.* **2006**, 2393–2405.
- [31] A search for P=P with the c.n. of P set to 2 yielded 113 hits (130 bonds) ranging from 1.985 to 2.159 Å with a mean of 2.04(3) Å. *Cambridge Structural Database, Version 5.41*, see also: F. H. Allen, *Acta Crystallogr. Sect. B* **2002**, 58, 380–388.
- [32] Search for Si–P single and double bonds in the CSD gave 36 hits ranging from 2.0630 to 2.1880 Å (mean 2.116 Å) for Si=P double bonds and 1052 hits ranging from 2.067 to 2.987 Å (mean 2.253 Å) for Si–P single bonds. C. R. Groom, I. J. Bruno, M. P. Lightfoot, S. C. Ward, *Acta Crystallogr. Sect. B Struct. Sci. Cryst. Eng. Mater.* **2016**, 72, 171–179.
- [33] V. Y. A. Lee, M. Kawai, A. Sekiguchi, H. Ranaivonjatovo, J. Escudé, *Organometallics* **2009**, 28, 4262–4265.
- [34] M. Driess, S. Rell, H. Pritzlow, R. Janoschek, *Angew. Chem. Int. Ed.* **1997**, 36, 1326–1329; *Angew. Chem.* **1997**, 109, 1384–1387.
- [35] M. K. Sharma, C. Wölper, G. Haberhauer, *Angew. Chem. Int. Ed.* **2021**, 60, 6784–6790; *Angew. Chem.* **2021**, 133, 6859–6865.
- [36] a) R. Damrauer, S. E. Pusey, *Organometallics* **2009**, 28, 1289–1294; b) T. Szilvási, T. Veszprémi, *Dalton Trans.* **2011**, 40, 7193–7200; c) M. Scheer, G. Baláz, A. Seitz, *Chem. Rev.* **2010**, 110, 4236–4256.
- [37] a) M. Scheer, U. Becker, M. H. Chisholm, J. C. Huffman, F. Lemoigno, O. Eisenstein, *Inorg. Chem.* **1995**, 34, 3117–3119; b) M. Scheer, U. Becker, J. Magull, *Polyhedron* **1998**, 17, 1983–1989; c) J. Bresien, K. Faust, A. Schulz, *Rev. Inorg. Chem.* **2022**, 42, 1–20.
- [38] a) S. Du, J. Yin, Y. Chi, L. Xu, W.-X. Zhang, *Angew. Chem. Int. Ed.* **2017**, 56, 15886–15890; *Angew. Chem.* **2017**, 129, 16102–16106; b) G. Luo, S. Du, P. Wang, F. Liu, W.-X. Zhang, Y. Luo, *Chem. Eur. J.* **2020**, 26, 13282–13287.
- [39] W. Lu, K. Xu, Y. Li, H. Hirao, R. Kinjo, *Angew. Chem. Int. Ed.* **2018**, 57, 15691–15695; *Angew. Chem.* **2018**, 130, 15917–15921.
- [40] X. Sun, A. Hinz, P. W. Roesky, *CCS* **2022**, 4, 1843–1849.

Manuscript received: April 5, 2022

Accepted manuscript online: May 30, 2022

Version of record online: June 23, 2022